Influence of Anchor Depth and Friction Coefficient Between Anchor and Rock on the Trajectory of Rock Masses Detachment

Józef Jonak[1], Robert Karpiński[1*], Andrzej Wójcik[1]

[1] Department of Machine Design and Mechatronics, Faculty of Mechanical Engineering, Lublin University of Technology, Nadbystrzycka 36, 20-618 Lublin, Poland

* Corresponding author's e-mail: r.karpinski@pollub.pl

ABSTRACT

This work presents the results of a FEA (Finite Element Analysis) concerning the propagation of the fracture trajectory during the detachment of rock masses. The analysis considers mechanical anchoring parameters, including the depth of anchoring and the friction between the anchor head and the brittle material. The analysis involved varying the effective anchorage depth h_{ef} = 50, 100, and 150 mm, along with considering different coefficients of friction (μ) for the anchor head against the rock, including 0.15, 0.3, and 0.45. The results indicated that within the chosen range of anchorage depths, the extent of damage increases with the depth of anchor embedment. However, the depth of anchoring, considering the studied range of this parameter and the assumed mechanical properties of the rock, did not have a significant effect on the value of the angle cone (α_0) during the initial phase of the medium's destruction. For the friction coefficient μ = 0.15, there is a clear deep penetration into the fracture at its initial stage of development (at the initial angle of α_0 = -20°), promoting further spread of the fracture on the free surface. For larger values of the friction coefficient (μ = 0.3 and 0.45) – the trend is less pronounced (α_0 = -2°÷-8°) resulting in a decrease in the crack range.

Keywords: rock, rock mechanics, mining, sandstone, rock, undercut anchors, FEM, friction, CCD, Abaqus

INTRODUCTION

Undercut anchors are used in the technology of embedding steel structural elements in concrete engineering structures [1–4]. This anchor, in installation form, is embedded in a previously prepared hole. The concrete is then undercut by simultaneously rotating the sleeve and gradually screwing it into the threaded part. The expansion sleeve elements supported by the "conical" anchor head then make an undercut in the concrete, leading to the installation of the anchor. The work conducted in this field has primarily concentrated on assessing the load capacity of anchors based on their design, the physical and mechanical characteristics of the installation medium, and the impact of installation techniques [5–7].

The process of optimization is facilitated by achieving a comprehensive understanding of the actual behavior of engineering structures through the combination of numerical modeling with data obtained from experimental studies [8–12]. Such an approach also affects the possibility of reducing the number of experiments and reducing the costs associated with conducting experiments, which is extremely important for analyses in field conditions [13–16]. Numerical methods, such as the FEM (finite element method) [17–20], BEM (boundary element method) [21,22], as well as deterministic and probabilistic methods, are now employed to analyze cracking problems in materials, including rock and concrete substrates (especially those reinforced with steel) [23–25].

The research aimed to develop technology for detaching rock blocks by pulling out pre-embedded undercutting anchors from the rock medium [26]. The analysis focused on the necessity of developing a mining method for rock

situations where conventional mechanical mining techniques might not be applicable. A significant limitation in using explosive mining was the existence of pulverized coal and methane, which could potentially lead to explosions [27,28].

So far, mechanical anchors, with different design and embedding technology, are mainly used in the assembly of steel structure elements in concrete objects [29,30]. For such applications, relevant standards have been developed [31,32], relevant mechanical models have been developed, and a model material failure under anchor action has been proposed [33]. The model assumes a simplification of the damage zone (Fig. 1), and more recently a simplification of the damage form in the form of a pyramidal [34] is assumed. In these models, it was assumed that the surface of the detachment (the formation of the destruction cone, is inclined at an angle α, equal to about 35° on average, in terms of free space The radius of the destruction zone on this surface is 3hef. The geometry of the rock failure model under the action of the anchor is illustrated in Figure 1.

Due to the proposed unconventional use of undercutting anchors in the process of detaching masses of rock, the authors of the study conducted a number of verification studies, which showed, among other things, that the course of destruction of weak rock is different than in concrete [35–37]. It was found, for example, that the shape and extent of the failure zone in rock are significantly different from that observed for concrete. The values of forces required to pull out an anchor embedded in a rock medium (for comparable depths of anchor embedment) are significantly higher than for concrete [38]. Preliminary results show, for example, that the diameter of the anchor head undercutting the rock, has no significant effect on the extent of the failure zone [39].
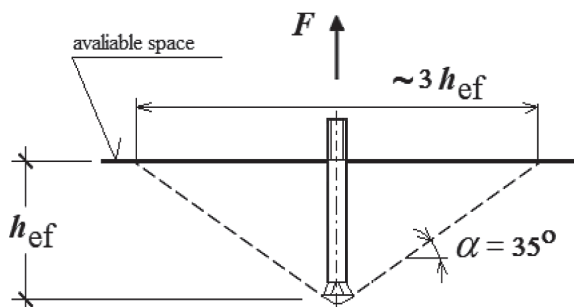
However, a number of issues remain that require further research, including, for example, the effect of the effective anchor depth – h_{ef} (Fig. 2 [40]), or friction of the head against the rock on the course of destruction and the interaction of the zones of destruction (as in Fig. 3). Preliminary numerical studies [40,41], over the range of anchorage depths studied, have shown no significant difference in the extent of detachment, despite the fact that literature reports [42,43] show that for concretes, an increase in the failure cone angle was observed as anchorage depth increased (Fig. 2).
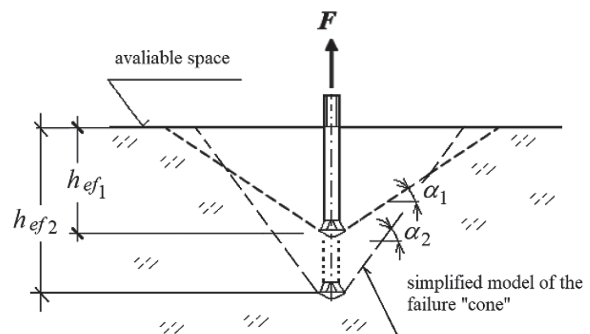
The effectiveness of the proposed method depends on the interaction of elementary destruction zones, as it influences the optimal sequence of drilling holes for anchors and, consequently, the potential volume of stripped rock. As a result, it affects the energy intensity of excavation of the proposed method. The clarification of these aspects justifies the research in the topic under discussion.

The main objective of this study was to numerically investigate the impact of the crucial technological parameters of anchoring, namely the effective anchorage depth (h_{ef}) and the friction value (μ) between the anchor and the rock formation. The study focused on determining their influence on the formation of the initial propagation angle (α_0), which is crucial for estimating the size of the damage zone. The tests were conducted in a homogeneous, continuous medium for a defined deposition depth and friction coefficient.

MATERIALS AND METHODS

Simulation conditions

The analysis was conducted under axisymmetric assumptions due to the geometry of the undercutting anchor, which greatly simplified the

Fig. 1. Simplified model of the destruction zone: F – the anchor pull-out force, h_{ef} – embedment depth, α – the angle of cone of destruction

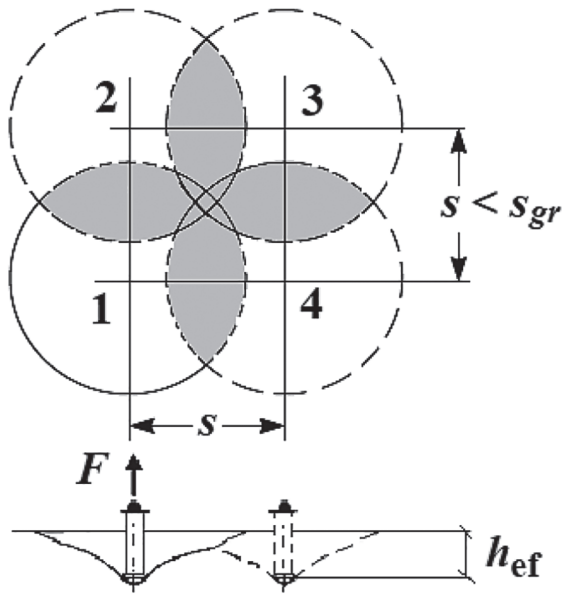**Fig. 2.** Effect of deposition depth on the extent of medium failure

Fig. 3. Hypothetical effect of anchor pullout sequence on the interaction of failure cones

numerical modeling process. The focus of the study was on the impact of the anchor limited to the conical anchor head with the rock. Other areas of the anchor in contact with the material were disregarded because, in practical situations, the anchor hole has a diameter slightly larger than the cylindrical part of the anchor by about 2 mm (1 mm on the radius of the hole). The analysis considered the effect of friction in the contact zone.

Effective anchorage depths equal to h_{ef} = 50, 100 and 150 mm were considered. The friction coefficient in the analysis equal to α = 0.15, 0.30, 0.45. The analysis was carried out using ABAQUS (Abaqus 2022) [44–46], which enables Finite Element Method (FEM) analysis. The XFEM algorithm was used to analyze the propagation of the failure (crack) surface. As per reference [47].

Model parameters

A 3D axis-symmetric model in the form of a cylinder was used, built by rotating the figure in Figure 4 (symmetry) [30], was considered in the analysis:
- radius of the rock model = 700 mm,
- height = 300 mm.

The model geometry was subjected to rotation around the anchor axis, leading to the establishment of a 3D representation of the rock medium in the anchor-rock contact zone, influenced by the anchor undercutting head. The analysis made use of half of this 3D model, as depicted in Figure 5.

Analysis of rock fracture propagation was carried out using the XFEM algorithm, available in ABAQUS. The preliminary model obtained for the use of the algorithm, is illustrated in Figure 6.

Boundary conditions

The FEM model nodes were subjected to restraints, where the three translational degrees of freedom U1=U2=U3=0 were imposed on the base and sidewalls, as illustrated in Figure 7.
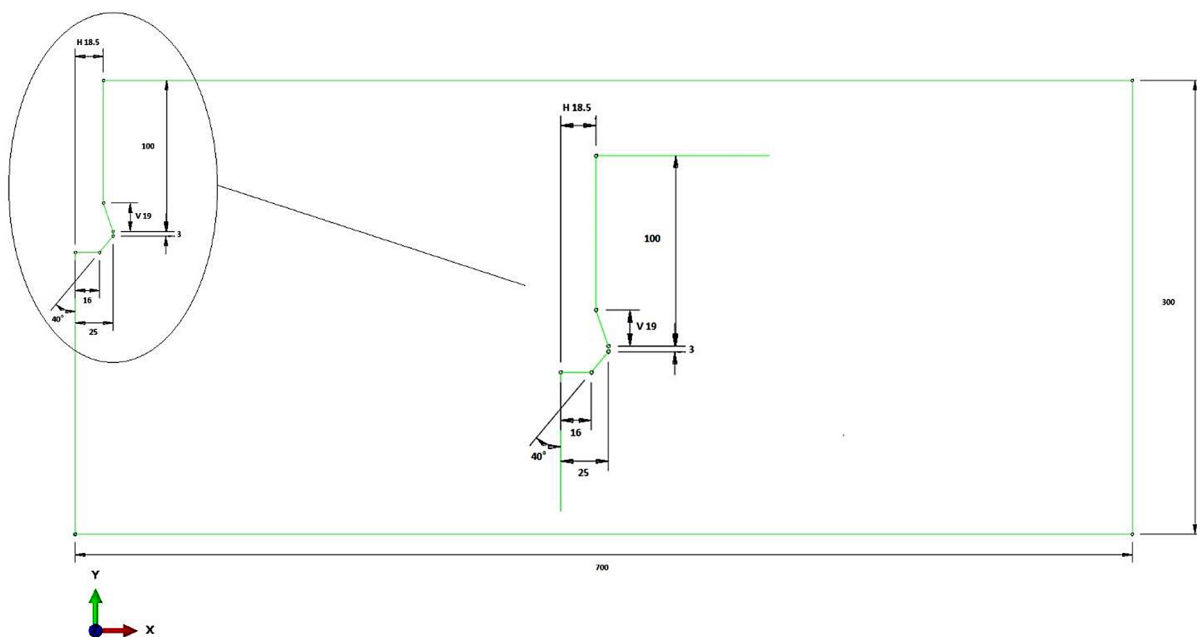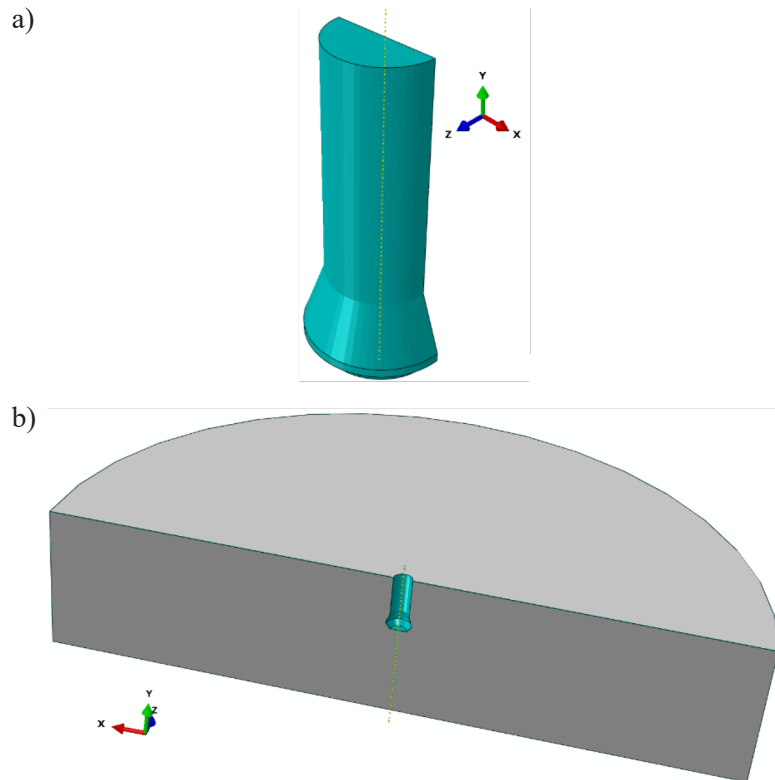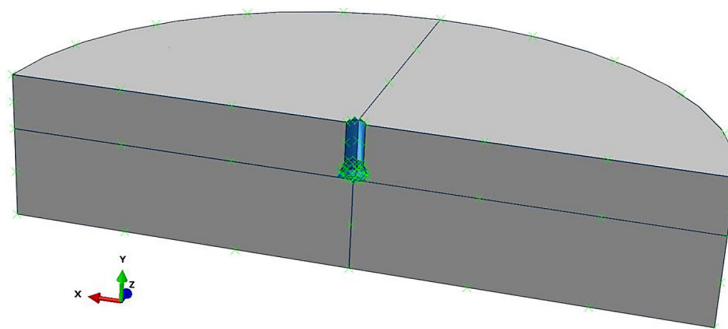

Fig. 4. Model of the rock medium (HILTI- HAD- M20 anchor)

a)

b)

Fig. 5. Undercut anchor surface model (a), and 3D (axis-symmetric) model
of rock medium with undercut anchor (1/2 model) (b)

Fig. 6. Initial discretization of the model to use the XFEM algorithm

The model has symmetry with respect to the XY plane, hence U3=UR1=UR2=0. A kinematic forcing was implemented on the anchor, resulting in vertical displacement along the Y-axis. The magnitude of displacement was systematically incremented with a predefined jump until the analysis was terminated.

Finite element mesh

The model's mesh was generated using hexagonal elements with a "sweep" algorithm, which is adapted to the model's shape. The mesh construction involved employing C3D8R elements.

These elements had a base linear dimension of 14 mm. The model's perimeter was divided with intervals of 10 degrees, as illustrated in Figure 8 and Table 1.

Mechanical parameters of the rock medium

- Young's modulus = 14276 MPa,
- Poisson's ratio = 0.247.

The MAXPS failure criterion (maximum principal (normal) stress criterion) was used: the maximum tensile stress in the principal direction for the rock medium was assumed = 7.74 MPa.
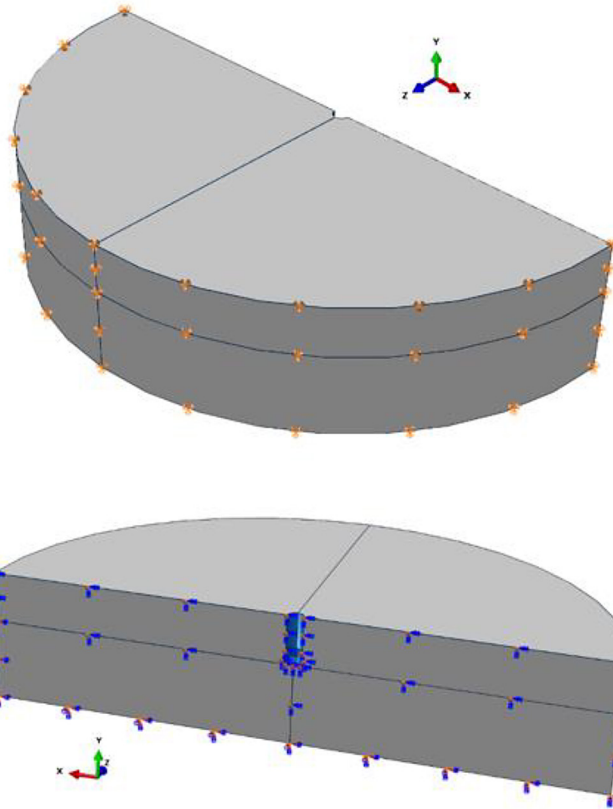
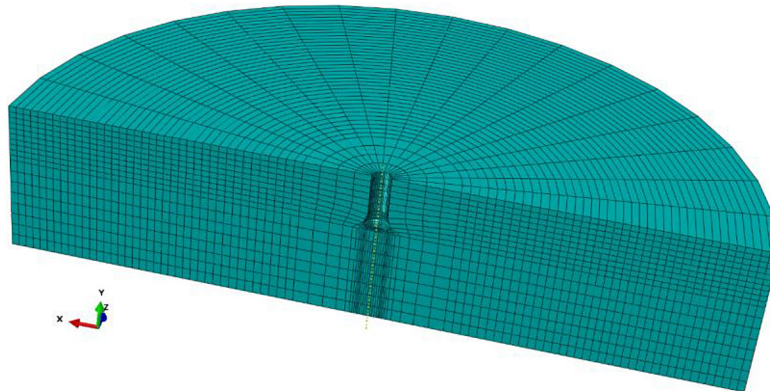**Fig. 7.** Restraints of boundary nodes of the rock medium model

Fig. 8. FEM of the rock medium model for one of the tested variants

Table 1. Characteristics of the obtained finite element meshes

Model	h_{ef} = 150	h_{ef} = 100	h_{ef} = 50
Number of nodes	17481	17351	16165
Number of elements	15300	15264	14112

The sub-option of ABAQUS "Damage evolution, type: Energy" was applied to the adopted MAXPS criterion, i.e., evolution based on energy, the value of which is the critical fracture energy in the 1st mode. The failure energy for the rock medium was assumed G_{fc} = 0.355 N/mm, distribution – linear.

A stabilization factor = 0.000001 was used in the calculations.

RESULTS

Figure 9 shows the result of simulating the propagation of the resulting crack (failure surface) for anchoring depths h_{ef} = 50, 100 and 150 mm, for a constant value of friction coefficient μ = 0.45.

a)

ODB: Brenna-3D-180_L50mi045.odb   Abaqus/Standard 2023   Wed Jul 19 11:24:23 Srodkowoeuropejski czas letni 2023   Step: Step-1
Increment   376: Step Time =   7.9105E-02

b)

ODB: Brenna-3D-180_L100mi045.odb   Abaqus/Standard 2023   Wed Jul 19 12:53:54 Srodkowoeuropejski czas letni 2023   Step: Step-1
Increment   1210: Step Time =   0.1708

c)

ODB: Brenna-3D-180_L150mi045.odb   Abaqus/Standard 2023   Tue Jul 18 20:58:13 Srodkowoeuropejski czas letni 2023   Step: Step-1
Increment   1005: Step Time =   0.2144

Fig. 9. Effect of effective anchorage depth h_{ef} on failure trajectory: h_{ef} = 50 mm, b) h_{ef} = 100 mm, c) h_{ef} = 150 mm, for friction coefficient μ = 0.45

The analysis demonstrated that within the chosen range of anchoring depth, the potential extent of the destruction zone, measured on the free surface relative to the anchor axis, increases with its augmentation. However, the depth of anchorage, considering the studied range of this parameter and the adopted mechanical parameters of the rock, does not significantly affect the value of the destruction cone angle ($\alpha 0$ - angle at the initial stage of the medium destruction, as shown in Fig. 10a). Due to the challenges posed by the XFEM algorithm in determining the direction of crack tip propagation in the last phase of propagation (before the crack reaches the free surface of the rock), it becomes impossible to ascertain the angle of the destruction cone for the complete trajectory of the crack. This is because, during this phase, the crack predominantly "circles" without reaching the free surface, and this phenomenon has been extensively analyzed in the study [48].

Conversely, Figure 10 demonstrates the impact of the coefficient of friction between the rock and the anchor head for an anchor depth of h_{ef}=150 mm.

As the analysis showed, for the simulation conditions adopted, i.e. a constant anchoring depth of h_{ef} = 150 mm and for the value of the friction coefficient assumed in the simulation, equal to μ = 0.15, 0.30, 0.45 there is a clear difference in the crack trajectory. For the value of the friction coefficient μ = 0.15, there is a clear deep penetration into the fracture at its initial stage of development (at the initial angle α_0 = -20°), favoring the further reach of the fracture on the free surface. For larger values of the coefficient of friction (μ = 0.3 and 0.45 as in Fig. 10b, c) – this tendency is less pronounced (α_0 = ~ -2° ÷ -8°) resulting in a reduction in the extent of the fracture. As a result, the volume of rock blocks being detached will be smaller than is the case for rocks with a lower coefficient of friction against the anchor head.

The results of the conducted tests, in the range of parameters adopted for simulation, coincide with the results of experimental studies [27,42], a
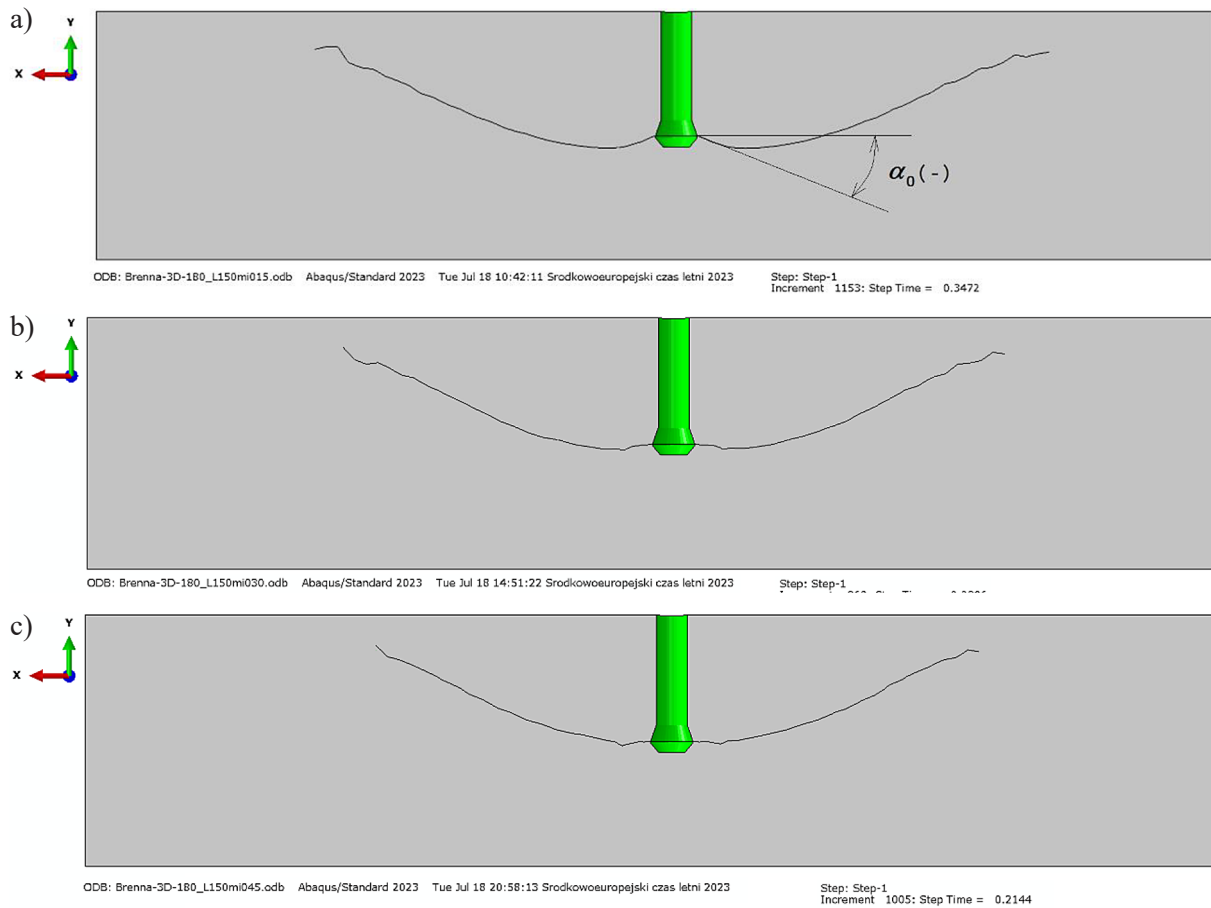
Fig. 10. Effect of the value of the coefficient of friction of the rock against the anchor head on the course of the failure trajectory: a) $\mu = 0.15$, b) $\mu = 0.30$, c) $\mu = 0.45$; for $h_{ef} = 150$ mm, α_0 – initial angle of crack propagation

summary of which is illustrated in Figure 11 [27]. This is especially true for the trend in the trajectory of fractures (failure surfaces) in the case of weak sandstones studied at the Brenna mine, whose mechanical parameters coincide with one of the simulation variants.

CONCLUSIONS

The issue of the influence of the depth of anchoring on the formation of the angle of the cone of destruction *a* and the shape of the fracture trajectory (which affects the potential volume
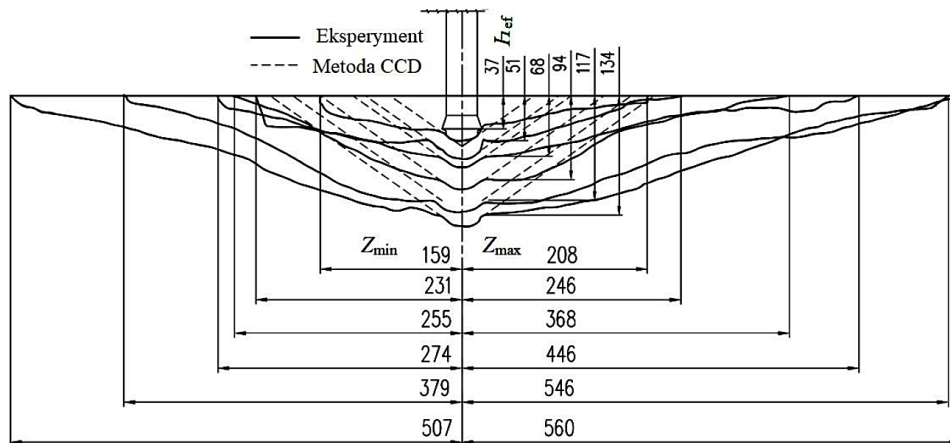
Fig. 11. Fracture trajectories (outline of the fracture surface in the axial section of the anchor) for different anchorage depths

of the stripped rock) is further an open question. Simulations showed a weak effect of anchorage depth (in the considered range of values of this parameter) on the extent of the fracture (failure surface) which slightly deviates from the signaled relationships found in concretes, especially for much larger anchorage depths than realized by studies [49,50] and realized by the presented numerical studies. However, the presented results of the study are consistent with the results of extensive research [51], where the dependence of the failure cone angle but on the anchor pull-out rate (the rate of inflicted deformation of the rock) was demonstrated, while no such dependence on the depth of anchorage was found.

REFERENCES

1. Bokor B, Sharma A, Hofmann J. Experimental investigations on concrete cone failure of rectangular and non-rectangular anchor groups. Engineering Structures. 2019 Jun;188:202–17.

2. Bokor B, Tóth M, Sharma A. Fasteners in steel fiber reinforced concrete subjected to increased loading rates. Fibers. 2018 Dec 6;6(4):93.

3. A. Al- Ta S, A. Mohammed A. Tensile strength of short headed anchors embedded in steel fibrous concrete. AREJ, 2010 Oct 28;18(5):35–49.

4. Ashour AF, Alqedra MA. Concrete breakout strength of single anchors in tension using neural networks. Advances in Engineering Software. 2005 Feb;36(2):87–97.

5. Pallarés L, Hajjar JF. Headed steel stud anchors in composite structures, Part I: Shear. Journal of Constructional Steel Research. 2010 Feb;66(2):198–212.

6. Pallarés L, Hajjar JF. Headed steel stud anchors in composite structures, Part II: Tension and interaction. Journal of Constructional Steel Research. 2010 Feb;66(2):213–28.

7. Brincker R, Ulfkjær JP, Adamsen P, Langvad L, Toft R. Analytical model for hook anchor pull-out. In: Proceedings of the International Symposium on Anchors in Theory and Practice: Salzburg, Austria, 9-10 october 1995. CRC Press/Balkema; 1995. p. 3–15.

8. Wysmulski P. Non-linear analysis of the postbuckling behaviour of eccentrically compressed composite channel-section columns. Composite Structures. 2023 Feb;305:116446.

9. Falkowicz K. Experimental and numerical failure analysis of thin-walled composite plates using progressive failure analysis. Composite Structures. 2023 Feb;305:116474.

10. Różyło P, Wysmulski P, Falkowicz K. Fem and experimental analysis of thin-walled composite elements under compression. International Journal of Applied Mechanics and Engineering. 2017;22(2).

11. Rogala M, Gajewski J. Crashworthiness analysis of thin-walled square columns with a hole trigger. Materials. 2023 Jun 5;16(11):4196.

12. Rogala M, Gajewski J, Gawdzińska K. Crashworthiness analysis of thin-walled aluminum columns filled with aluminum–silicon carbide composite foam. Composite Structures. 2022 Nov;299:116102.

13. Rogala M, Gajewski J, Górecki M. Study on the Effect of geometrical parameters of a hexagonal trigger on energy absorber performance using ANN. Materials. 2021 Oct 11;14(20):5981.

14. Wysmulski P. Numerical and experimental study of crack propagation in the tensile composite plate with the open hole. Adv Sci Technol Res J, 2023;17(4). http://www.astrj.com/Numerical-and-Experimental-Study-of-Crack-Propagation-in-the-Tensile-Composite-Plate,169970,0,2.html

15. Falkowicz K, Dębski H, Wysmulski P, Różyło P. The behaviour of compressed plate with a central cut-out, made of composite in an asymmetrical arrangement of layers. Composite Structures. 2019 Apr;214:406–13.

16. Rogala M, Tuchowski W, Czarnecka-Komorowska D, Gawdzińska K. Analysis and assessment of aluminum and aluminum-ceramic foams structure. Adv Sci Technol Res J, 2022;16(4). http://www.astrj.com/Analysis-and-assessment-of-aluminum-and-aluminum-ceramic-foams-structure,153028,0,2.html

17. Falkowicz K. Experimental and numerical analysis of compression thin-walled composite plates weakened by cut-outs. Archives of Civil Engineering. 2017 Dec 1;63(4):161–72.

18. Rozylo P, Falkowicz K, Wysmulski P, Debski H, Pasnik J, Kral J. Experimental-numerical failure analysis of thin-walled composite columns using advanced damage models. Materials. 2021 Mar 19;14(6):1506.

19. Falkowicz K. Numerical onvestigations of perforated CFRP Z-cross-section profiles, under axial compression. Materials. 2022 Oct 3;15(19):6874.

20. Wysmulski P. The effect of load eccentricity on the compressed CFRP Z-shaped columns in the weak post-critical state. Composite Structures. 2022 Dec;301:116184.

21. Romero A, Galvín P, Domínguez J. 3D non-linear time domain FEM–BEM approach to soil–structure interaction problems. Engineering Analysis with Boundary Elements. 2013 Mar;37(3):501–12.

22. Romero A, Galvín P, Tadeu A. An accurate treatment of non-homogeneous boundary conditions for development of the BEM. Engineering Analysis with Boundary Elements. 2020 Jul;116:93–101.

23. Jendzelovsky N, Tvrda K. Probabilistic Analysis of a hospital building slab foundation. Applied

Sciences. 2020 Nov 6;10(21):7887.

24. Jendzelovsky N, Tvrda K. Analysis of a bending-stressed pile in interaction with subsoil. Buildings. 2023 Jun 9;13(6):1497.

25. Foraboschi P. Ultimate shear force of an any anchor group post-installed into concrete. Materials. 2023 Mar 24;16(7):2608.

26. Siegmund M, Jonak J. Analysis of the process of loosening the rocks with different strength properties using the undercutting bolts. IOP Conf Ser: Mater Sci Eng. 2019 Dec 1;679(1):012014.

27. Jonak J, Siegmund M, Karpiński R, Wójcik A. Three-dimensional finite element analysis of the undercut anchor group effect in rock cone failure. Materials. 2020 Mar 15;13(6):1332.

28. Cebula D, Kalita M, Prostański D. Underground tests of rescue tunnel driving technology by the method of rock destruction. Mining Machines, 2015, 33(1). http://yadda.icm.edu.pl/baztech/element/bwmeta1.element.baztech-fdd70e92-71df-4f2b-8f47-3541fe40207f

29. Eligehausen R, Mallée R, Silva JF. Anchorage in concrete construction. Berlin: Ernst; 2006. 378 p.

30. HILTI. Technisches Handbuch der Befestigungstechnik für Hoch- und Ingenieurbau. Ausgabe; HILTI: Schaan, Liechtenstein,. 2016.

31. Committee 355 ACI. Evaluating the performance of post-installed mechanical anchors in concrete (ACI 355.2-01) and commentary (ACI 355.2 R-01): An ACI Standard. American Concrete Institute; 2002.

32. Gontarz J, Podgórski J, Jonak J, Kalita M, Siegmund M. Comparison between numerical analysis and actual results for a pull-out test. Available from: http://et.ippt.pan.pl/index.php/et/article/view/1005

33. Fuchs W, Eligehausen R, Breen J. Concrete capacity design (CCD) approach for fastening to concrete. Aci Structural Journal. 1995;92:73–94.

34. SS-EN 1992-4 Eurocode 2-Design of Concrete Structures-Part 4: Design of Fastenings for Use in Concrete; SIS: Stockholm, Sweden; 2018.

35. Jonak J, Karpiński R, Wójcik A, Siegmund M. The influence of the physical-mechanical parameters of rock on the extent of the initial failure zone under the action of an undercut anchor. Materials. 2021 Apr 8;14(8):1841.

36. Jonak J, Karpiński R, Wójcik A. Influence of the undercut anchor head angle on the propagation of the failure zone of the rock medium. Materials. 2021 May 2;14(9):2371.

37. Jonak J, Karpiński R, Wójcik A. Influence of the undercut anchor head angle on the propagation of the failure zone of the rock medium – Part II. Materials. 2021 Jul 12;14(14):3880.

38. Jonak J, Karpiński R, Siegmund M, Machrowska A, Prostański D. Experimental verification of standard recommendations for estimating the load-carrying capacity of undercut anchors in rock material. Advances in Science and Technology Research Journal, 2021 Jan 11; http://www.astrj.com/Experimental-Verification-of-Standard-Recommendations-for-Estimating-the-Load-carrying,132279,0,2.html

39. Jonak J, Karpiński R, Wójcik A, Siegmund M. The effect of undercut anchor diameter on the rock failure cone area in pullout tests. Adv Sci Technol Res J. 2022 Nov 1;16(5):261–70.

40. Jonak J, Karpiński R, Wójcik A. Numerical analysis of the effect of embedment depth on the geometry of the cone failure. J Phys: Conf Ser. 2021 Dec 1;2130(1):012012.

41. Jonak J, Karpiński R, Wójcik A, Siegmund M, Kalita M. Determining the effect of rock strength parameters on the breakout area utilizing the new design of the undercut/breakout anchor. Materials. 2022 Jan 23;15(3):851.

42. Bennett MS. Prediction of the shear cone geometry surrounding headed anchor studs. 1979;

43. Jonak J, Karpiński R, Wójcik A, Siegmund M. Numerical investigation of the formation of a failure cone during the pullout of an undercutting anchor. Materials. 2023 Feb 28;16(5):2010.

44. Falkowicz K. Validation of extension-bending and extension-twisting coupled laminates in elastic element. Adv Sci Technol Res J. 2023 Jun 6;17(3):309–19.

45. Falkowicz K. Numerical buckling analysis of thin-walled channel-section composite profiles weakened by cut-outs. Adv Sci Technol Res J. 2022 Dec 1;16(6):88–96.

46. Wysmulski P. Failure mechanism of tensile CFRP composite plates with variable hole diameter. Materials. 2023 Jun 29;16(13):4714.

47. Bazant ZP, Kazemi MT, Hasegawa T, Mazars J. Size effect in Brazilian split-cylinder tests. Measurements and fracture analysis. ACI Materials Journal. 1991;88(3):325–32.

48. Gontarz J. Modelowanie propagacji szczeliny w materiałach kruchych. Lublin: Politechnika Lubelska. Wydawnictwo; 2022. 189 p. (Monografie / Politechnika Lubelska).

49. Jonak J, Karpiński R, Wójcik A. Numerical analysis of undercut anchor effect on rock. J Phys: Conf Ser. 2021 Dec 1;2130(1):012011.

50. Jonak J, Karpiński R, Siegmund M, Wójcik A, Jonak K. Analysis of the rock failure cone size relative to the group effect from a triangular anchorage system. Materials. 2020 Oct 19;13(20):4657.

51. Al Saeab L. Finite element modelling of anchorage to concrete systems at different strain rates. Ottawa, Ontario: Carleton University; 2019. https://repository.library.carleton.ca/concern/etds/gh93h020x